PERGAMON

Mechanism and Machine Theory 35 (2000) 1117–1139

MECHANISM AND MACHINE THEORY

www.elsevier.com/locate/mechmt

On the workspace, assembly configurations and singularity curves of the *RRRRR*-type planar manipulator

J. Jesús Cervantes-Sánchez*, J. Cesar Hernández-Rodríguez, J. Gabriel Rendón-Sánchez

University of Guanajuato, F.I.M.E.E., Department of Mechanical Engineering, Prolongación Tampico S/N 36730, Col. Bellavista, Salamanca, Gto., Mexico

Received 28 July 1999; accepted 29 July 1999

Abstract

In this paper, a broadly applicable approach for numerically obtaining the workspace and the singularity curves of a planar *RRRRR*-type manipulator is presented. The workspace generation is formulated as a direct kinematic problem involving only two branches which are mathematically defined and related with the manipulator's assembly configurations. For solving that problem, the analytical solution of two simple quadratic equations is found. A simple existence criterion is also obtained to detect the set of points forming the manipulator's workspace. On the other hand, the singularity curves are composed of sets of singular points. In order to obtain the singular points, the properties of the Jacobian matrix are used. The complete method has been implemented and tested, as illustrated with examples for different geometrical properties of the manipulator. For each of these examples, the corresponding singularity curves are graphically generated to obtain the practical manipulator's workspace. This feature is a very powerful design tool which is indispensable in visualizing and analyzing the kinematic working capability of the manipulator. © 2000 Elsevier Science Ltd. All rights reserved.

1. Introduction

One of the early attempts for obtaining a robotic device was certainly the four-bar linkage,

* Corresponding author. Tel.: +52-4648-0911; fax: +52-4647-2400.
E-mail address: jecer@salamanca.ugto.mx (J.J. Cervantes-Sánchez).

0094-114X/00/$ - see front matter
PII: S0094-114X(99)00061-0

which has only one degree of freedom. Its main robotic applications were focused to the rigid body guidance [1,2] and trajectory generation [3,4]. Although there was a lot of research [1–4], the main drawback of this linkage was the limited and small number of precision poses (configurations of the coupler bar) and precision points (locations of a point fixed on the coupler bar) reached by the mechanism.

Detecting the necessity of having a robotic device with a more versatile working capability, an additional freedom was needed, another link was added and a five-bar linkage was then obtained. A five-bar linkage requires two inputs because of it has two degrees of freedom. When these input motions are given by two rotary actuators, the mechanism has two actuated joints and three unactuated joints and it is called *controllable* [5]. Controllable means that the mechanism can find the finite actuator torques to maintain static equilibrium against any finite external load (force and/or moment) exerted on any point or any link of the mechanism. If the two input rotary motions can be controlled independently, the five-bar linkage is then transformed to a programmable linkage or a robotic device which is known as five-bar *RRRRR*-type planar manipulator. This robot can be used for positioning a point on a region of a plane which is known as *workspace*. On this workspace, there exist singular points where the manipulator is out of control and excessive forces and/or moments are generated in the links, joints and actuators. For that reason, the singular points are dangerous in the operation of the robot. These points divide the workspace into multiple regions [6]. Therefore, in the robot design, the geometrical properties of the manipulator must be taking into account so that, considering the singular points, the manipulator can have a practical workspace which includes the prescribed workspace. Also, in the operation of the manipulator, the effector should be driven through trajectories which are designed to avoid all singular points.

Because of the variety of motions permitted by the kinematic structure of the five-bar linkage, it is an exciting and challenging mechanism which has motivated the realization of several researches including the development of classification schemes [7,8], mobility criterion [9,10], modes of configuration [11], acceleration maps [12], solution space and atlas of the reachable workspace [13], a study of the workspace [14] and a centro-based characterization of singularities in the workspace [15]. Entering in more detail, in [13], the workspace of a planar *RRRRR* manipulator has been studied using geometry. This led to an exhaustive list of geometric conditions under which such workspaces are obtained. However, from a design point of view, it is desirable to develop a tool that will allow to obtain easily the workspace of an arbitrary manipulator. In other words, given a set of lengths of the manipulator's links, provide the designer with a graphical representation of the workspace. Such a result could be very difficult to obtain using only geometrical methods. On the other hand, the method proposed in [15] requires the determination of the centroes at each configuration of the manipulator and also, the reported classification of singularities depends on the special purpose employed notation, i.e. one needs to translate the proposed singularity for understanding its physical implication. Finally, the study presented in [14] is intended for obtaining only the workspace of a point which is not the end effector considered here.

This paper presents a novel, simple and powerful method of analysis for numerically generating the workspace and the singularity curves of the *RRRRR* planar manipulator which is based on the existence of the analytical solutions of two simple quadratic equations and the determinant of the Jacobian matrix of the manipulator. This simultaneous formulation can be

very helpful for the designer by allowing the superposition of the workspace and the singularity locus. Moreover, as will be seen presently, the generation of the workspace and the singularity curves is automatic, i.e. it does not require the previous knowledge of numerous geometrical relationships between link-lengths, a kinematic inversion, extreme values of rotability angles, modes of configuration and the determination of the centroes of the manipulator.

2. Description of the *RRRRR* planar manipulator

A symmetrical *RRRRR* planar manipulator is shown in Fig. 1. This manipulator is a closed loop mechanism with parallel topology, i.e. it has an arrangement in which ground-based actuators work in parallel when positioning an end effector. Two actuated revolute (*R* type) joints are driven by two independent motors which give the rotary input motions, θ_1 and θ_2, of the input links *OA* and *DB*, respectively. The both motors are fixed to the base link, *OD* link, at point *O* and point *D*. The lengths of the links *OA*, *OD* and *DB* are denoted by *l*, *d* and *l*, respectively. Additional to the base link and the two active links, there are two other links which are connected to links *OA* and *DB* by passive (unactuated) revolute joints located at points *A* and *B*. Finally, the passive links *AP* and *BP* are joined by another passive revolute joint located at point *P* and close the kinematic loop. The lengths of the links *AP* and *BP* are denoted by *L* and *L*, respectively. For the purposes of this paper, it is assumed that the links are coplanar and do not interact to each other. Also, the point *P* represents the end effector or operation point of the robotic device.

The coordinates (x,y) of the operation point are represented with reference to the coordinate

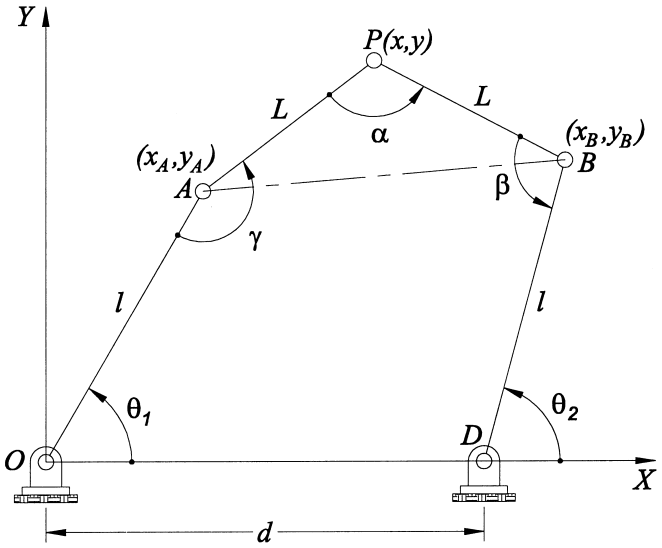

Fig. 1. Kinematic diagram of a planar *RRRRR* manipulator.

axes fixed at point O, where the X axis is directed along the base link. These cartesian coordinates are the output motion of the manipulator and they depend only on the independent angular motions θ_1 and θ_2. It must be noticed that the angles γ, α and β represent the angular motions of the passive revolute joints and, for that reason, one can not have control on them, i.e. they only can attain those values permited by the input motions θ_1 and θ_2. In a rigorous sense, these last two ideas can help to explain the difference between a five-bar *mechanism* and a five-bar *manipulator*, i.e. all the links of a mechanism can be theoretically moved to any configuration (satisfying the kinematic constraints imposed by the revolute joints) whereas this reasoning is only valid for the active links of the manipulator.

3. Formulation of the mathematical model

From the geometry shown in Fig. 1, it can be noticed the triangle APB, which is now isolated and presented in Fig. 2.

Refering to Fig. 2, for every reachable configuration of the manipulator, the distance between points A and P and P and B can be expressed in a vectorial form, respectively, as:

$$(\mathbf{p}-\mathbf{a})\cdot(\mathbf{p}-\mathbf{a}) = L^2 \tag{1}$$

$$(\mathbf{p}-\mathbf{b})\cdot(\mathbf{p}-\mathbf{b}) = L^2 \tag{2}$$

where $\mathbf{p} = (x,y)^T$, $\mathbf{a} = (x_A,y_A)^T$ and $\mathbf{b} = (x_B,y_B)^T$ are, respectively, the position vectors of the points P, A and B.

In order to deal with simpler equations, the scalar form of the Eqs. (1) and (2) can be obtained by using the Cartesian components of vectors **p**, **a** and **b**. This leads to:

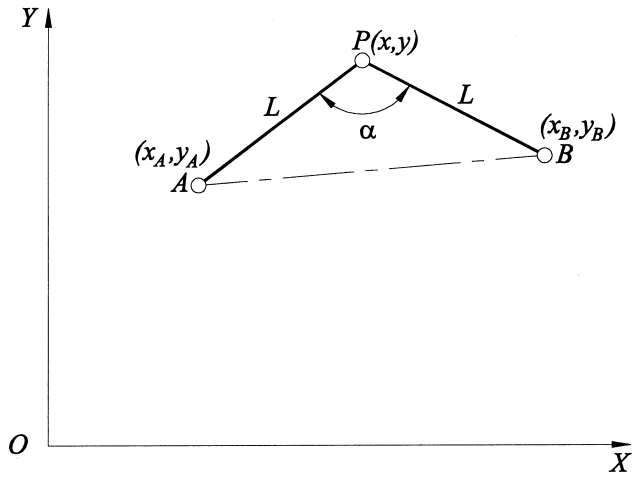

Fig. 2. Isolated triangle APB.

$$(x - x_A)^2 + (y - y_A)^2 = L^2 \tag{3}$$

$$(x - x_B)^2 + (y - y_B)^2 = L^2 \tag{4}$$

The above equations are simply the equations of two circles centered at points A and B, respectively. Moreover, the quadratic form of Eqs. (3) and (4) can be written as:

$$x^2 + y^2 - (2x_A)x - (2y_A)y + x_A^2 + y_A^2 - L^2 = 0 \tag{5}$$

$$x^2 + y^2 - (2x_B)x - (2y_B)y + x_B^2 + y_B^2 - L^2 = 0 \tag{6}$$

Because of the simplicity of Eqs. (5) and (6), they have an analytical solution, as it will be shown later. Hereafter, these equations will be called *quadratic equations*.

4. Solution of the mathematical model

The analytical solution of the quadratic equations can be obtained as follows. Substracting Eqs. (6) from (5), one obtains:

$$2(x_B - x_A)x + 2(y_B - y_A)y + R - S = 0 \tag{7}$$

where: $R \equiv x_A^2 + y_A^2$ and $S \equiv x_B^2 + y_B^2$.

Now, an expression for x can be obtained from (7). This is given by:

$$x = My + N \tag{8}$$

where the coefficients M and N are defined as:

$$M \equiv \left(\frac{y_A - y_B}{x_B - x_A}\right)$$

$$N \equiv \frac{1}{2}\left(\frac{S - R}{x_B - x_A}\right)$$

Now, from the substitution of expression (8) into Eq. (5), a well known second order equation for y is obtained:

$$ay^2 + by + c = 0 \tag{9}$$

where the coefficients a, b and c are given by:

$$a \equiv (M^2 + 1)$$

$$b \equiv 2(MN - Mx_A - y_A)$$

$$c \equiv (N^2 - 2Nx_A + R)$$

Solving Eq. (9) for y, one obtains the two well known possible solutions given, respectively, by:

$$y_1 = \frac{-b + \sqrt{b^2 - 4ac}}{2a} \tag{10}$$

能否从机械设计上保证一定有解？
这样不用考虑可能带来的机械结构毁坏

$$y_2 = \frac{-b - \sqrt{b^2 - 4ac}}{2a} \tag{11}$$

如果某个AB组合，无解，机械结构会被破坏

Now, knowing the above presented values of y_1 and y_2, two values for x can be also obtained using Eq. (8):

$$x_1 = My_1 + N \tag{12}$$

$$x_2 = My_2 + N \tag{13}$$

Because of the quadratic nature of Eqs. (5) and (6), it leads to a maximum of two solutions. The graphical representation of them is shown in Fig. 3. Both solutions produce two branches, which are symmetric with respect to the AB axis. Resorting to Eqs. (3) and (4), the solution can be also considered as the intersection of two circles.

Before leaving this section, it is worth noticing that the above solution is based completely on the knowledge of the Cartesian coordinates of points A and B. As will become evident later, these coordinates can be expressed as functions of the input motions produced by the actuators of the manipulator, which are assumed to be known, e.g. by means of a rotary encoder. Obviously, it also depends on the lengths of the links, which can be easily modified to investigate their influence on the workspace of the manipulator.

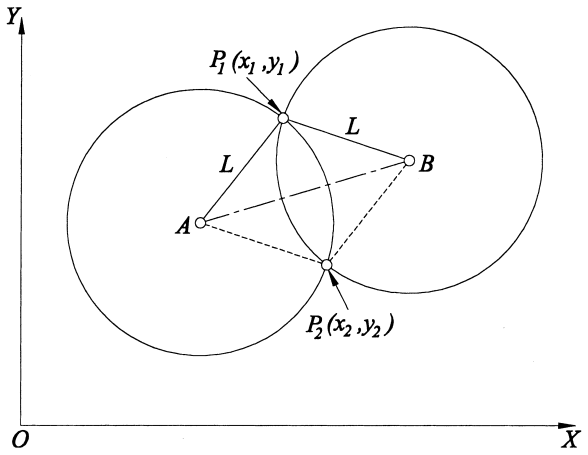

Fig. 3. Graphical representation of the obtained solutions.

4.1. The existence criterion of a nonvanishing workspace

One important criterion for the usefulness of the manipulator is that we have a nonvanishing workspace. According to the way in which the foregoing solution was found, for a given endpoint of the manipulator to have existence for prescribed input variables, the expression under the square root in Eqs. (10) and (11) has to be positive. Thus, the points forming the workspace, will be those for which the following criterion is valid:

$$(b^2 - 4ac) \geq 0 \tag{14}$$

该判别式用于判断AB组合是否产生在WS中的点。
如果(θ1,θ2)满足该判别式，对应的(x,y)在WS中画出。数值上很容易画出WS.

It is noticed that the above imposed condition for a workspace point is very simple and it can be easily implemented in a computer program.

4.2. Solution cases

Analyzing the Eqs. (7) and (8), it can be noticed that when $x_A = x_B$, the solution given by (10), (11), (12) and (13) will be indefinite. For that reason, it is necessary to find an alternative solution for this case. Substituting the condition $x_A = x_B$ in Eq. (7) and after some algebraic manipulation, one can obtain:

$$y = \tfrac{1}{2}(y_A + y_B) \tag{15}$$

Moreover, substituting now Eq. (15) in Eq. (5), arranging terms and simplifying, it is obtained that:

$$x_1 = x_A + \sqrt{L^2 - \left(\frac{y_A - y_B}{2}\right)^2} \tag{16}$$

$$x_2 = x_A - \sqrt{L^2 - \left(\frac{y_A - y_B}{2}\right)^2} \tag{17}$$

For this particular case, the solution is then given by Eqs. (15), (16) and (17). From these equations, it can be noticed that the solution includes only one value for y and two values for x, i.e. the solutions are symmetrical about an axis (parallel to the Y axis) which passes through the points A and B. The logic sense of it can be explained using Fig. 4 as reference.

Another particular case of a not defined solution occurs when $x_B = x_A$ and $y_B = y_A$ simultaneously. In this case, the points A and B are in coincidence and the circle Eqs. (3) and (4) are centered at the same point, i.e. one equation is exactly above the other one. Since the solution is now the intersection of two coincident circles, the operation point $P(x, y)$ can be located anywhere along the dashed circumference shown in Fig. 5.

As will be seen presently, the solution curve shown in Fig. 5 is closely related with the singularity curve which is obtained when the links AP and BP are aligned.

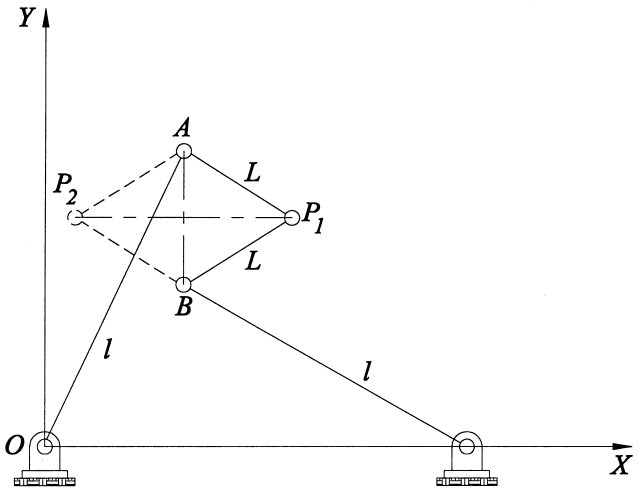

Fig. 4. Graphical representation of the solution when $x_B = x_A$.

4.3. Branching effects

Although the solution procedure above presented does not involve kinematic inversion, it leads to a branching problem. Branching in the *RRRRR* planar manipulator occurs when, for a given configuration of the input links, *OA* and *BD*, there exist two possible sets of configurations of the dependent links, *AP* and *BP*, i.e. two solutions $\mathbf{p}_1 = (x_1, y_1)^T$ and $\mathbf{p}_2 =$

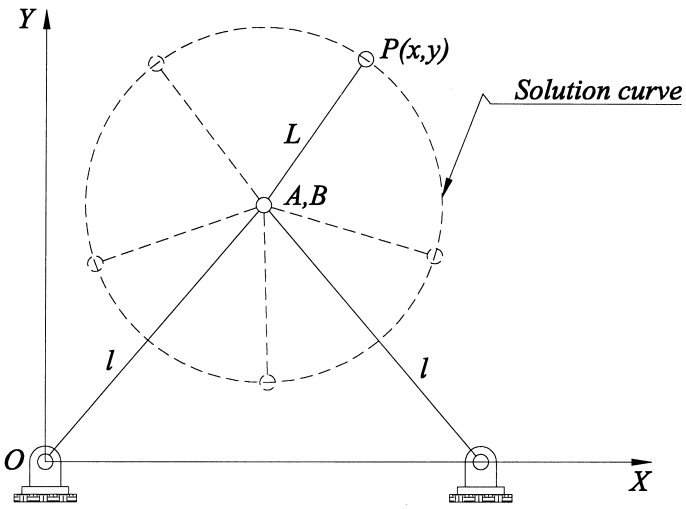

Fig. 5. Graphical representation of a non-defined solution.

$(x_2,y_2)^T$ for the location of the operation point are obtained. Unfortunately, each branch does not correspond always to one particular Eqs. (10) or (11) and the problem of branching can not be eliminated only by choosing one single equation as in the similar case of the synthesis of a four-bar linkage [16]. Therefore, it is necessary to choose the solutions so that the manipulator remains on the same branch, the procedure being then capable of avoiding undesirable branching effects.

A branching in a mechanism can physically move from one branched configuration to another configuration only by passing through a singular configuration [17]. Consequently, the mechanism must be disassembled and reassembled in order for it to pass through the singular configuration. This fact can be explained by using Fig. 6 as reference.

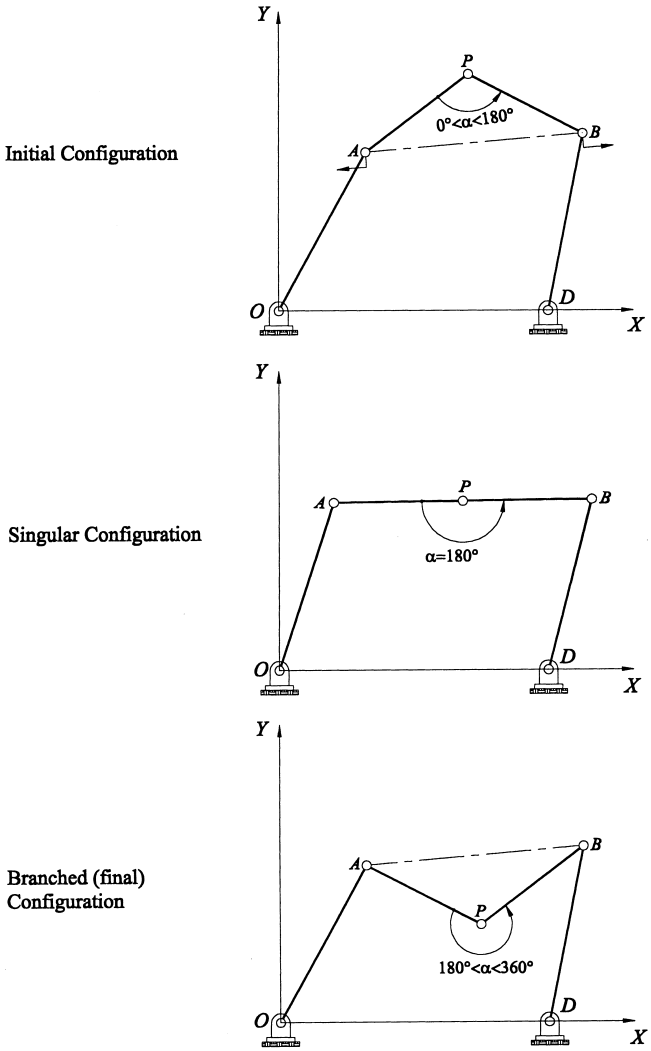

Fig. 6. Description of branching in the *RRRRR* planar manipulator.

The case of branching shown in Fig. 6 involves the pass through a singular configuration which is attained when $\alpha = 180^\circ$. In fact, the branched configuration can be considered as the reflection of the initial location of the point P about the AB axis. Also, it can be noticed that the configuration of the input links remains unchanged for both, the initial configuration and the final (branched) configuration shown in Fig. 6.

Now, the branching of the planar *RRRRR* manipulator can be mathematically formulated as follows. Referring to Fig. 6, we first define $\mathbf{u} \equiv (\mathbf{a}-\mathbf{p})$ and $\mathbf{v} \equiv (\mathbf{b}-\mathbf{p})$ as the relative-position vectors directed from P to A and from P to B, respectively. Moreover, the cross product of $\mathbf{u}$ and $\mathbf{v}$ can be stated as:

$$\mathbf{u} \times \mathbf{v} = \det(\mathbf{M})\hat{\mathbf{n}} \tag{18}$$

where $det(\cdot)$ is used to denote the *determinant* of $(\cdot)$ and the 2×2 matrix $\mathbf{M}$ is defined as:

$$\mathbf{M} \equiv [\mathbf{u}\ \mathbf{v}] \tag{19}$$

and $\hat{\mathbf{n}}$ is a unit vector perpendicular to both $\mathbf{u}$ and $\mathbf{v}$ according to the *right-hand rule*. Now, using the well known definition [18] given by:

$$\mathbf{u} \times \mathbf{v} \equiv (uv \sin\alpha)\hat{\mathbf{n}} \tag{20}$$

where $u \equiv ||\mathbf{u}||$ and $v \equiv ||\mathbf{v}||$ are the magnitudes of the vectors $\mathbf{u}$ and $\mathbf{v}$, respectively. Finally, combining (18) and (20), one can obtain:

$$\sin\alpha = \frac{\det(\mathbf{M})}{uv} \tag{21}$$

From a careful examination of Fig. 6, it can be noticed that for the interval $(0^\circ < \alpha < 180^\circ)$ the manipulator is on one branch and for $(180^\circ < \alpha < 360^\circ)$ the manipulator is on the other branch. Taking this fact into account, the value of α can be used to define the branch and therefore, by comparing this quantity at every configuration, we can ensure that the manipulator remains on the same branch. Moreover, knowing that for $(0^\circ < \alpha < 180^\circ)$ the $sin\,\alpha$ function is *positive* and for $(180^\circ < \alpha < 360^\circ)$ the $sin\ \alpha$ function is *negative*, it can be explained the equivalence between the branching identification proposed in this paper and the branching identification reported in [19]. However, since the inverse trigonometric function arcsine$(\cdot)$ is *double valued*, one needs to look for a single-valued function in the 0° to 360° range. In order to do it, the following procedure is presented. The *cosine* of α can be obtained in terms of the above described vectors $\mathbf{u}$ and $\mathbf{v}$ by the expression:

$$\cos\alpha = \frac{\mathbf{u} \cdot \mathbf{v}}{uv} \tag{22}$$

Now, the unique value of the α angle, which is defined by Eqs. (21) and (22) can be found [20] simply as follows:

$$\alpha = 2\arctan\left(\frac{\sin\alpha}{1+\cos\alpha}\right) \tag{23}$$

Obviously, when $\cos\alpha = -1$, then the above expression cannot be used, but in that case, the value is $\alpha = 180^\circ$.

4.4. Assembly configurations

Closely related to the branching, are the *assembly configurations*. In this paper, an assembly configuration is that kinematic configuration at which the planar *RRRRR* manipulator was initially assembled. Since we need to choose the solutions so that the manipulator remains on the same branch, the definition of the next two assembly configurations can be useful for branching identification purposes:

1. *Up configuration*. This configuration is attained when the angle between the dependent links (Fig. 6) is on the interval ($0^\circ < \alpha < 180^\circ$).
2. *Down configuration*. The planar *RRRRR* manipulator is on this configuration when the angle between the dependent links (Fig. 6) is on the interval ($180^\circ < \alpha < 360^\circ$).

It is worth noticing that with the aid of the above presented definitions, it is possible to present in a simplified form to the four modes of configuration reported in [11]. In fact, the mode 1 and the mode 2 can be considered as up configurations whereas the mode 3 and the mode 4 are down configurations.

5. Generation of the manipulator's workspace

For the purposes of this paper, a manipulator's workspace will be considered as an envelope which includes all reachable positions of the endpoint of the manipulator using all available input motions produced by the actuators. In order to obtain the workspace, the following procedure is proposed here. The workspace will be generated by means of two families of contour lines which are obtained by plotting the locations of the operation point of the manipulator in a $X-Y$ plane which results by varying one input variable and fixing other input variable. Moreover, as it was presented before, we need also to choose the assembly configuration (up or down) so that the manipulator remains on the same branch. Then, in this paper, the *up configuration* will be selected arbitrarily.

θ1 [0,360°] θ2 [0,360°]

Based on Fig. 1, one can obtain the Cartesian coordinates of points A and B in terms of the input motions θ_1 and θ_2. They are given by:

$$x_A = l\cos\theta_1 \tag{24}$$

$$y_A = l\sin\theta_1 \tag{25}$$

$$x_B = d + l\cos\theta_2 \tag{26}$$

$$y_B = l\sin\theta_2 \tag{27}$$

Substituting (24)–(27) into Eqs. (10)–(13), it can be noticed that the solutions depend on the input motions θ_1 and θ_2 and also on the lengths of the links.

Taking into account the above presented procedure, an interactive graphical tool has been developed in a computer package written specifically for the *RRRRR* planar manipulator. As a first example, the geometrical properties proposed in [13] are now considered. The obtained workspace is shown in Fig. 7. Comparing the workspace shown in Fig. 7 with the workspace reported in ([13], Fig. 8), several differences on the shape of the workspace can be detected. Such differences can be explained by means the following fact: it seems to be that the workspace presented in [13] was generated only by a simple geometric construction without the consideration of the assembly configurations, i.e. it was obtained considering only the planar *RRRRR* device as a *mechanism* instead of a *manipulator*. These differences can be also verified analyzing the boundary singularities shown presently in Fig. 14.

Other examples of the workspaces obtained with the proposed package are shown in Figs.

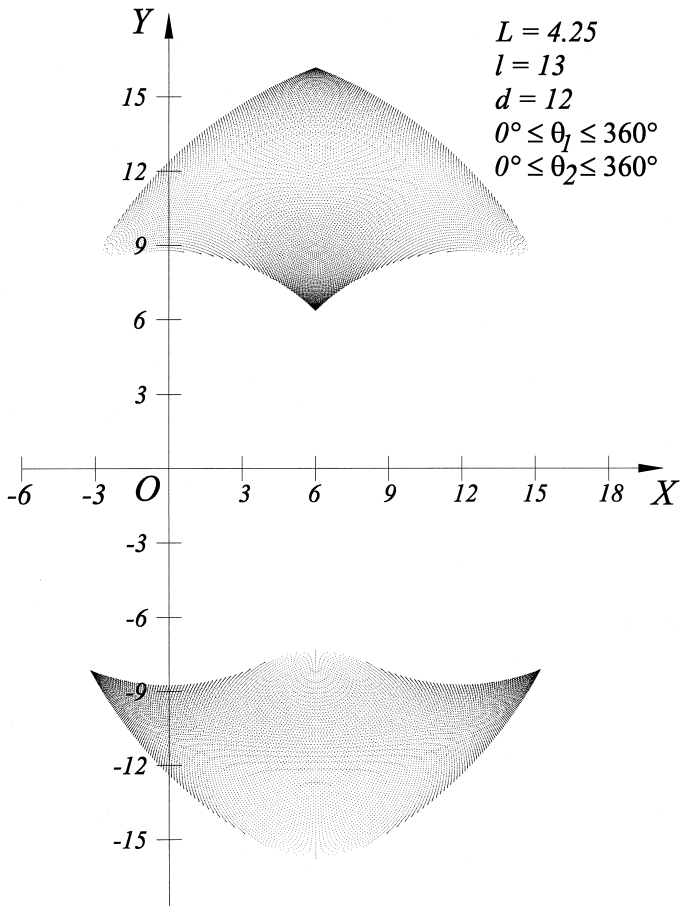

Fig. 7. Workspace for the geometrical properties reported in ([13], Fig. 8).

8–12. From these intricate figures, it can be noticed the power and versatility of the proposed method.

6. Singularity analysis

Because of the large number of configurations permitted by the kinematic structure of the planar *RRRRR* manipulator, a kinematic analysis of it leads inevitably to the problem of singular configurations. These configurations are defined as those in which the Jacobian matrix involved, i.e. that matrix relating the input speeds with the output speeds, is singular or indefinite.

6.1. Jacobian matrix

In order to obtain the Jacobian matrix of the manipulator under study, the following schematic diagram and procedure are proposed.

Refering to Fig. 13, the end point coordinates, x and y are given by:

$$x = L\cos\theta_1 + l\cos\phi_1 \tag{28}$$

$$y = L\sin\theta_1 + l\sin\phi_1 \tag{29}$$

Now, for maintaining closed the kinematic chain, the following constraint equations must be satisfied:

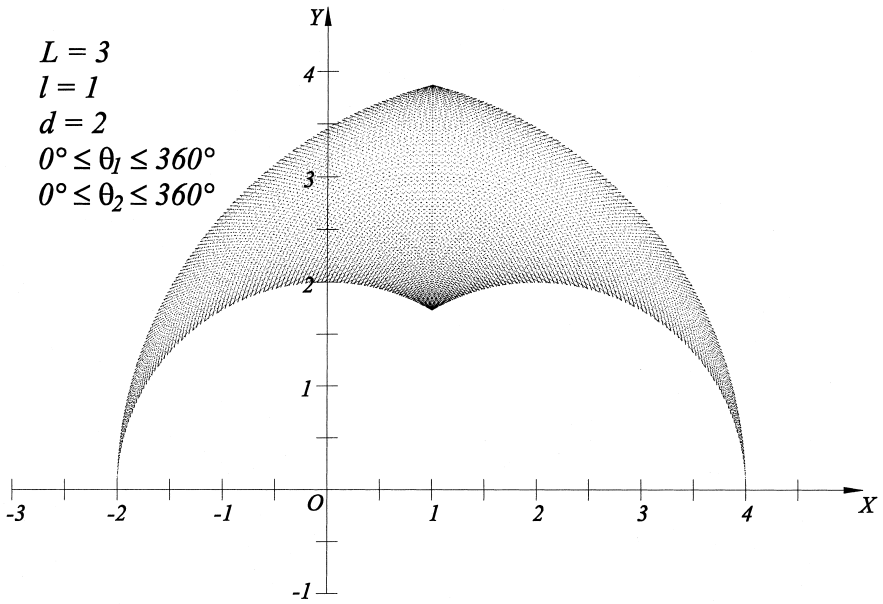

Fig. 8. Example of workspace for the geometry proposed in ([15], Fig. 5a).

$$L\cos\theta_1 + l\cos\phi_1 = d + L\cos\theta_2 + l\cos\phi_2 \tag{30}$$

$$L\sin\theta_1 + l\sin\phi_1 = L\sin\theta_2 + l\sin\phi_2 \tag{31}$$

这4个式子中l, L应互换

Differentiating Eqs. (28), (29), (30) and (31) with respect to time and eliminating $\dot{\phi}_1$ and $\dot{\phi}_2$, one obtains the relationship between the vector of output velocities $\dot{\mathbf{p}} = (\dot{x},\dot{y})^T$ and the vector of input velocities $\dot{\mathbf{q}} = (\dot{\theta}_1,\dot{\theta}_2)^T$:

$$\dot{\mathbf{p}} = [J]\dot{\mathbf{q}} \tag{32}$$

where the Jacobian matrix $[J]$ is given by:

主动杆长度

$$[J] = \frac{-l}{\sin(\phi_2-\phi_1)}\begin{bmatrix} \sin\theta_1\sin(\phi_2-\phi_1) + \sin\phi_1\sin(\theta_1-\phi_2) & -\sin\phi_1\sin(\theta_2-\phi_2) \\ -\cos\theta_1\sin(\phi_2-\phi_1) - \cos\phi_1\sin(\theta_1-\phi_2) & \cos\phi_1\sin(\theta_2-\phi_2) \end{bmatrix} \tag{33}$$

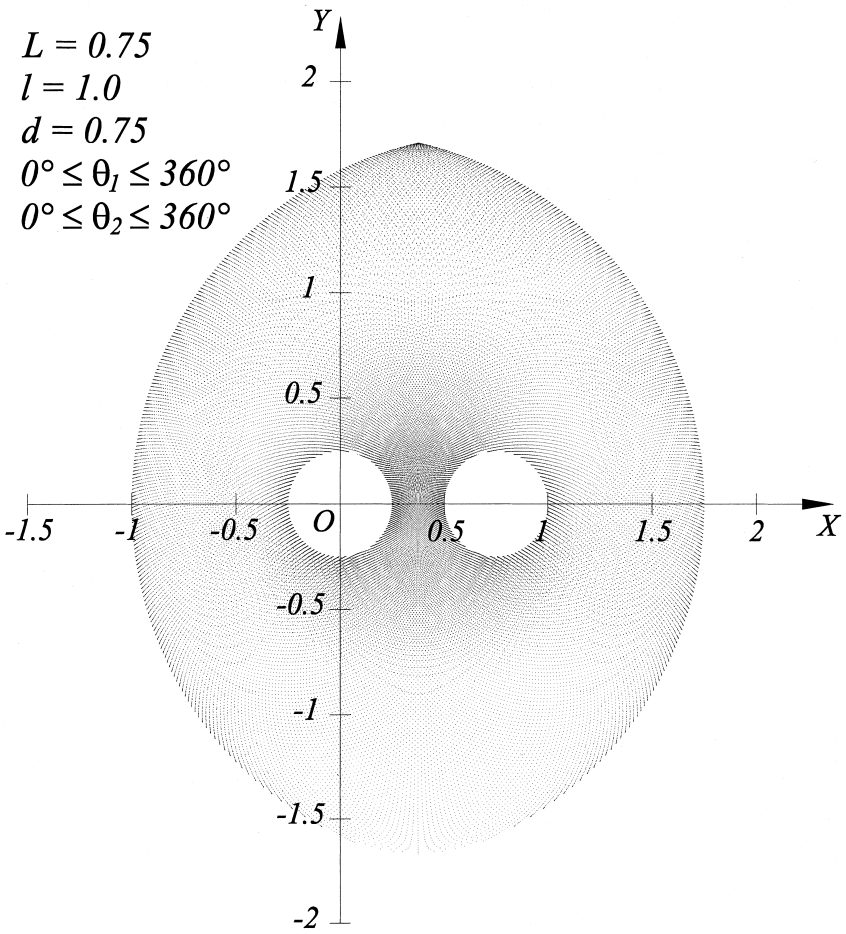

Fig. 9. Example of workspace for $L = 0.75$, $l = 1.0$, $d = 0.75$, $0^\circ \le \theta_1 \le 360^\circ$ and $0^\circ \le \theta_2 \le 360^\circ$.

6.2. Singularity conditions

In order to physically identify and mathematically formulate the singularity conditions of the planar *RRRRR* manipulator shown in Fig. 13, the determinant of the Jacobian matrix (33) is first obtained. Thus we find that it is given by:

$$\det(J) = l^2\left(\frac{\sin(\theta_1 - \phi_1)}{\sin(\phi_2 - \phi_1)}\right)\sin(\theta_2 - \phi_2) \tag{34}$$

In the above expression, there exist two conditions at which the determinant goes to zero, namely:

(a) $\sin(\theta_1 - \phi_1) = 0$
(b) $\sin(\theta_2 - \phi_2) = 0$

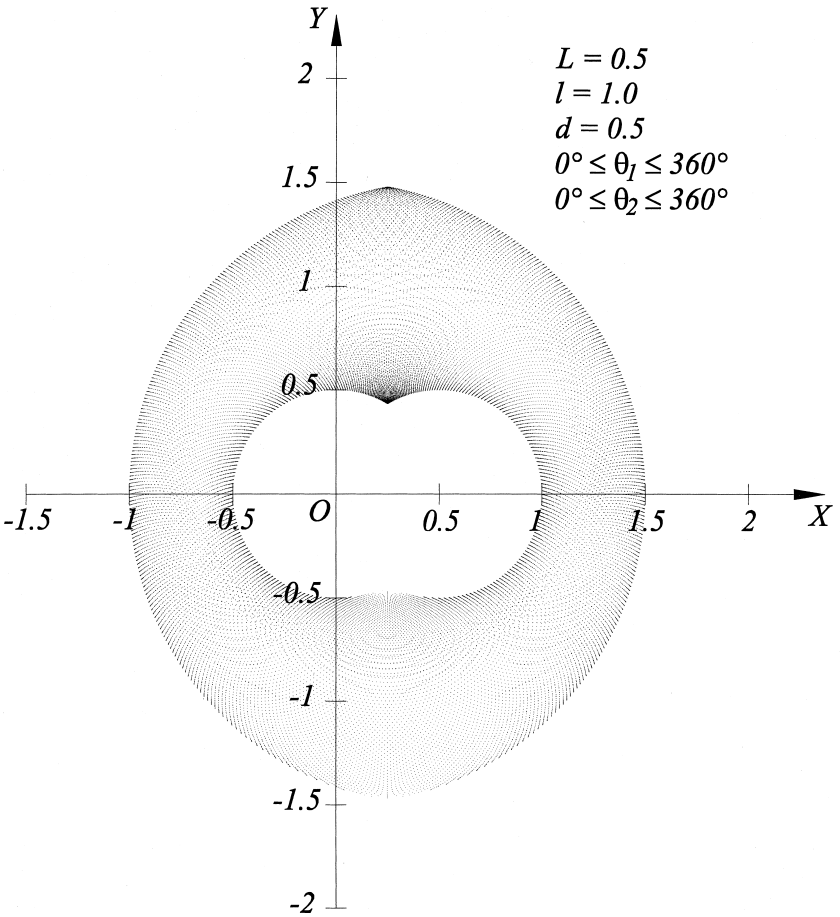

Fig. 10. Example of workspace for $L = 0.5$, $l = 1.0$, $d = 0.5$, $0^\circ \le \theta_1 \le 360^\circ$ and $0^\circ \le \theta_2 \le 360^\circ$.

(30,31)线性相关

From Eq. (33) it is found that the Jacobian matrix does not exist, i.e. this is indefinite, when the next condition is satisfied:

(c) $\sin(\phi_2 - \phi_1) = 0$.

The condition (a) implies that $\phi_1 = \theta_1$ or $\phi_1 = (\theta_1 + 180^\circ)$ for the supposed mobilities ($0^\circ \leq \phi_1 \leq 360^\circ$) and ($0^\circ \leq \theta_1 \leq 360^\circ$). Physically, when this condition is satisfied, the links OA and AP are aligned and the corresponding configuration is one in which the manipulator reaches either an external boundary of its workspace or an internal boundary.

On the other hand, the condition (b) implies that $\phi_2 = \theta_2$ or $\phi_2 = (\theta_2 + 180^\circ)$ for the supposed mobilities ($0^\circ \leq \phi_2 \leq 360^\circ$) and ($0^\circ \leq \theta_2 \leq 360^\circ$). For this condition, the links BD and BP are aligned and their configurations correspond to the limits of the workspace.

Finally, the condition (c) is satisfied when $\phi_2 = \phi_1$ or $\phi_2 = (\phi_1 + 180^\circ)$ for the supposed mobilities ($0^\circ \leq \phi_1 \leq 360^\circ$) and ($0^\circ \leq \phi_2 \leq 360^\circ$). In this case, the links AP and BP are aligned and the corresponding configurations are directly related with the indefinite solution which was presented previously (Fig. 5) and also with the intermediate singular configuration shown in Fig. 6. In fact, it can be noticed from Figs. 6 and 13 that the α angle can be expressed in terms of the difference ($\phi_2 - \phi_1$).

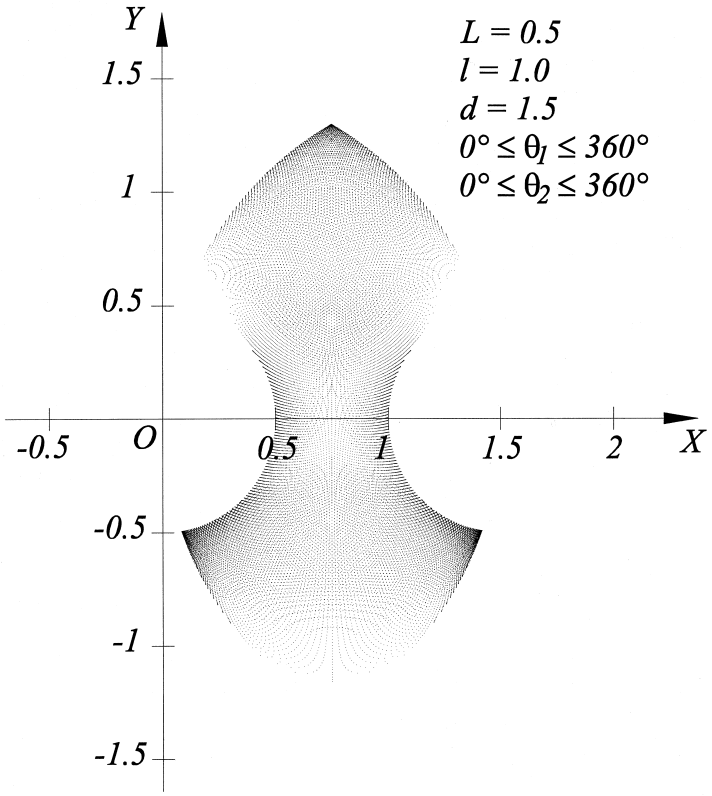

Fig. 11. Example of workspace for $L = 0.5$, $l = 1.0$, $d = 1.5$, $0^\circ \leq \theta_1 \leq 360^\circ$ and $0^\circ \leq \theta_2 \leq 360^\circ$.

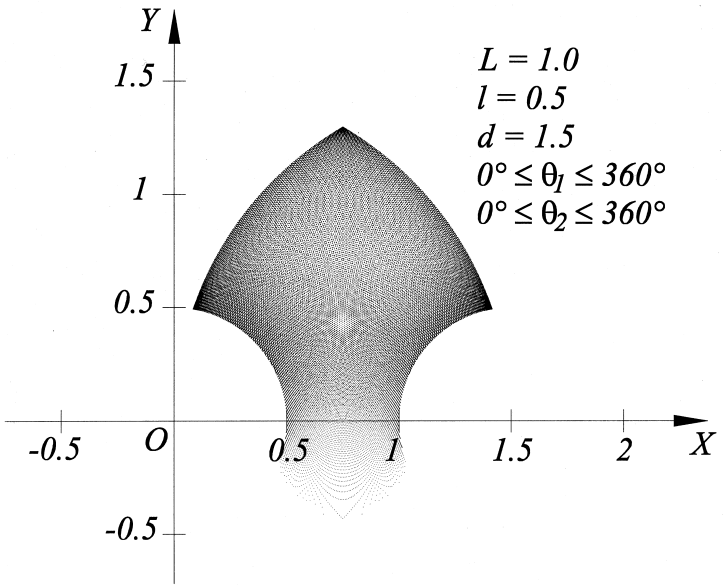

Fig. 12. Example of workspace for $L = 1.0$, $l = 0.5$, $d = 1.5$, $0^\circ \leq \theta_1 \leq 360^\circ$ and $0^\circ \leq \theta_2 \leq 360^\circ$.

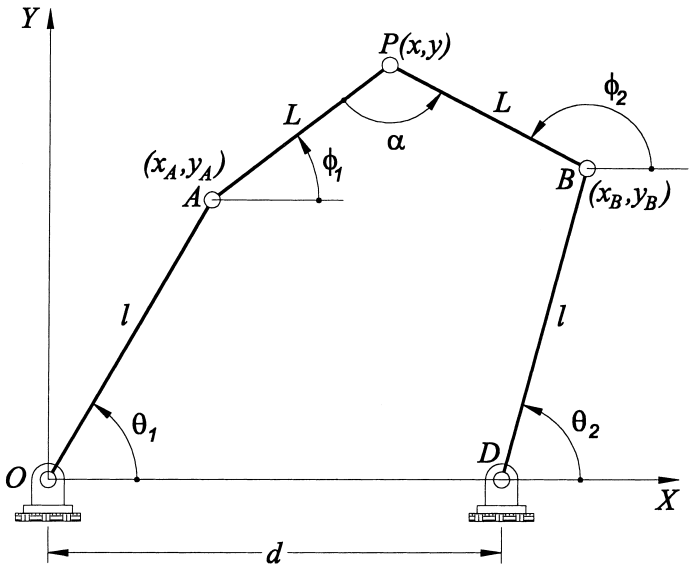

Fig. 13. Kinematic diagram for obtaining the Jacobian matrix.

6.3. Singular points and singularity curves

As it was seen previously, the singular points are dangerous in the operation of the manipulator and for that reason, one needs to avoid such points. A *singular point* is reached when the previously presented singular conditions (a), (b) or (c) are fulfilled. The sets of such singular points form in turn a set of curves called *singularity curves*. These curves are of a great importance because of that they divide the total workspace of the manipulator into smaller regions. Since the location of a singular point will be done by the computer package, i.e. each singular point will be numerically located, a specific procedure is required. Thus, a singular point is defined as a point which satisfies the following condition:

$$cond = 0 \qquad \text{(a) (b) (c)均是判定==0} \qquad (35)$$

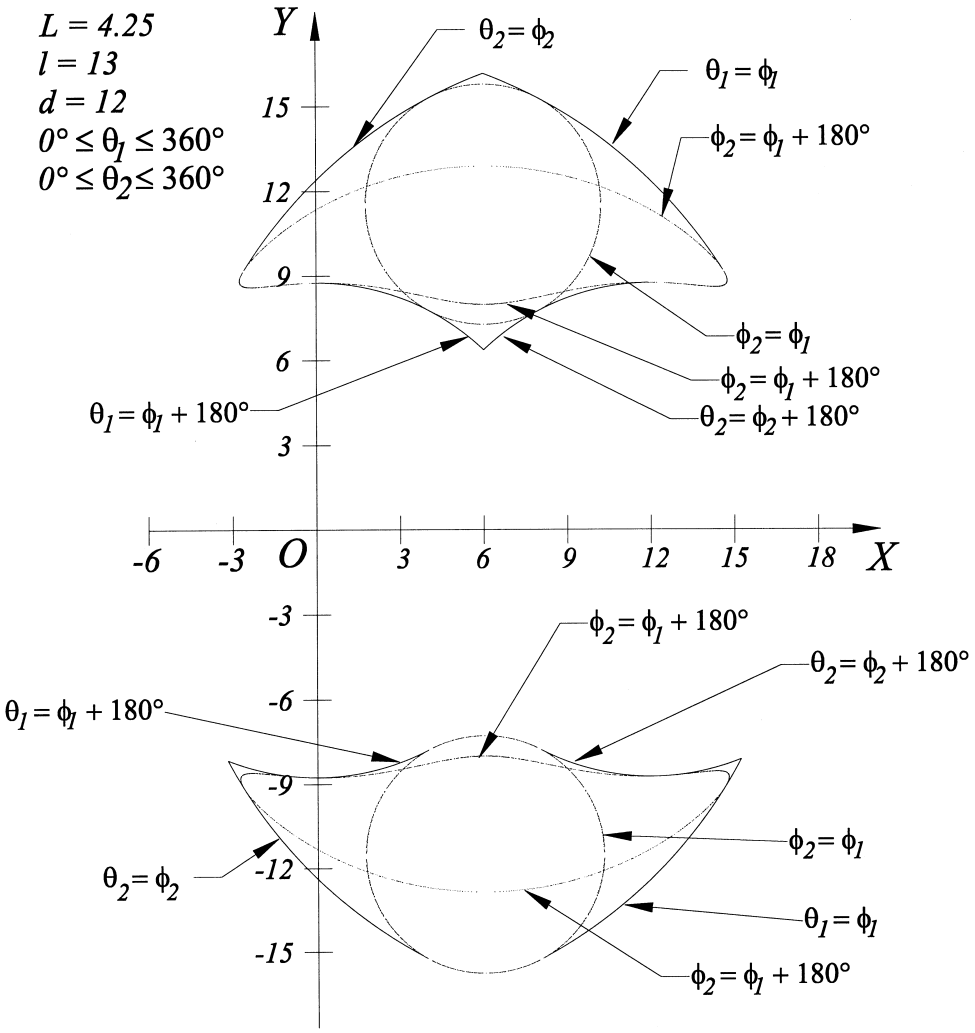

Fig. 14. Singularity curves for the geometrical properties reported in ([13], Fig. 8).

WS in Fig.7

where the term *cond* is used to represent any of the functions involved in the (a), (b) or (c) singular conditions previously presented in Section 6.2. When a point with $cond = 0$ is being numerically located, the definite point $cond = 0$ cannot be obtained and a point with $cond \simeq 0$ is obtained in practice. In this location procedure, the range which can be approximately identified with zero should be defined and whether or not there is really a singular point near the located point with $cond \simeq 0$ should be confirmed. Moreover, the procedure can be improved as follows. A point is determined as a singular point if the condition $cond \simeq 0$ is satisfied and the sign of the determinant of the Jacobian matrix changes when the output point is moved through it. According to the method proposed here, almost all the singular points can be determined very quickly and precisely.

是否存在在Curve外的点cond≈0 ???

???如何编程 through the point

In order to obtain the singularity curves based on a broadly applicable numerical formulation, aided by computer graphics, an interactive program was written specifically for the planar *RRRRR* manipulator.

The first example considered here, is that reported in ([13], Fig. 8). For This example, the obtained singularity curves are shown in Fig. 14. This figure can be used for explaining the differences on the shape of the workspace which were previously mentioned in Section 5.

The next example was taken from ([15], Fig. 5). For this example, the singularity curves shown in Fig. 15, were obtained using the above mentioned program. From this figure, it is evident that *internal singularities* (singularities located within the workspace) were found. This kind of singularity was obtained considering the singularity condition $\sin(\phi_2 - \phi_1) = 0$. Surprisingly, Sen and Mruthyunjaya [15] did not detect it in their reported work.

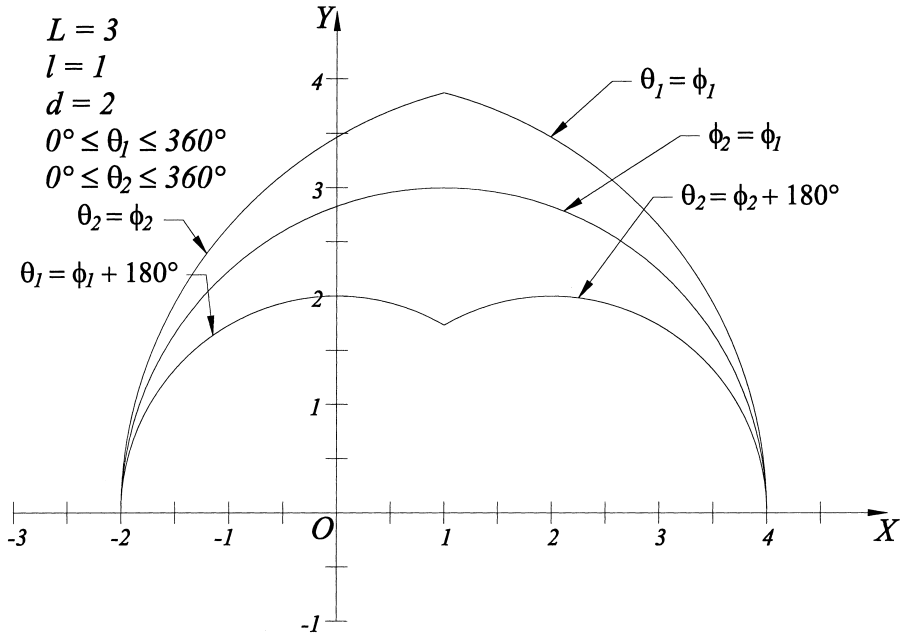

Fig. 15. Singularity curves for the geometrical properties reported in ([15], Fig. 5).

WS in Fig.8

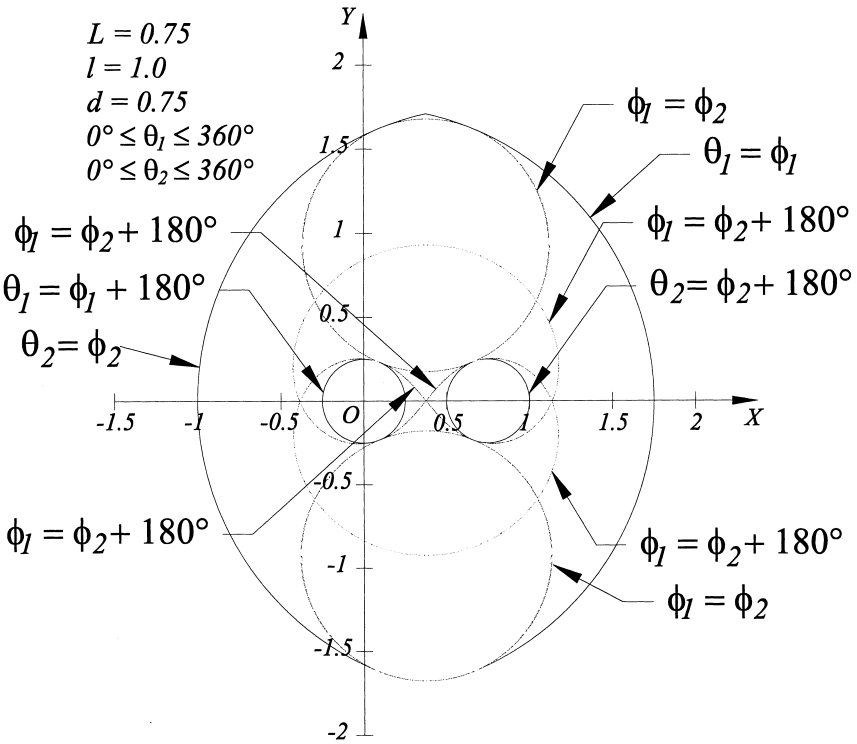

WS in Fig.9

Fig. 16. Singularity curves for $L = 0.75$, $l = 1.0$, $d = 0.75$, $0^\circ \le \theta_1 \le 360^\circ$ and $0^\circ \le \theta_2 \le 360^\circ$.

Other examples of results obtained with the here proposed program, are shown presently in Figs. 16–19.

Before leaving this section, it is worth noticing that the intricate curves previously shown, were automatically generated by the program proposed here.

7. Conclusions

A method for numerically obtaining the workspace and the singularity curves of a planar *RRRRR* manipulator has been presented. Its formulation is simple since it does not rely on complicated mathematical schemes. In fact, it was formulated as a direct kinematic problem which does not require a generally more complicated kinematic inversion and it is based only on two simple quadratic equations and their analytical solution. Also, the approach is broadly applicable because of that it has been implemented and tested as illustrated with examples for different geometrical properties of the manipulator. Moreover, it does not require a previous and exhaustive list of geometric conditions for obtaining the results, i.e. it is automatic. This latest feature helps also to obtain intricate workspaces and singularity curves which are difficult to get using only geometrical methods. Additionally, the method is efficient since it is founded on a very easy to evaluate existence criterion and the involved mathematical expressions for

(14)

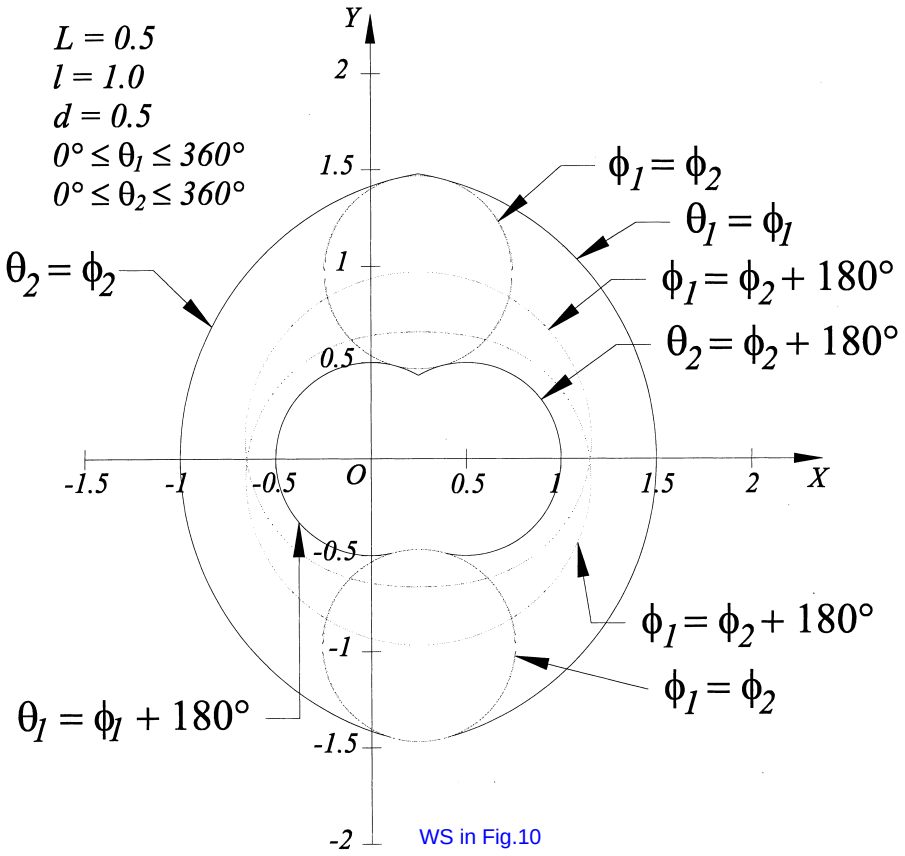

Fig. 17. Singularity curves for $L = 0.5$, $l = 1.0$, $d = 0.5$, $0^\circ \le \theta_1 \le 360^\circ$ and $0^\circ \le \theta_2 \le 360^\circ$.

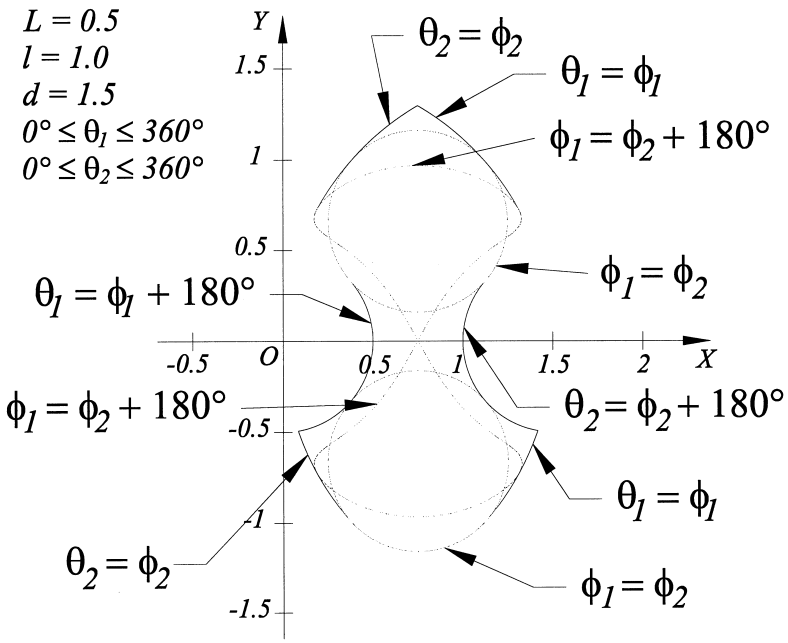

Fig. 18. Singularity curves for $L = 0.5$, $l = 1.0$, $d = 1.5$, $0^\circ \le \theta_1 \le 360^\circ$ and $0^\circ \le \theta_2 \le 360^\circ$.

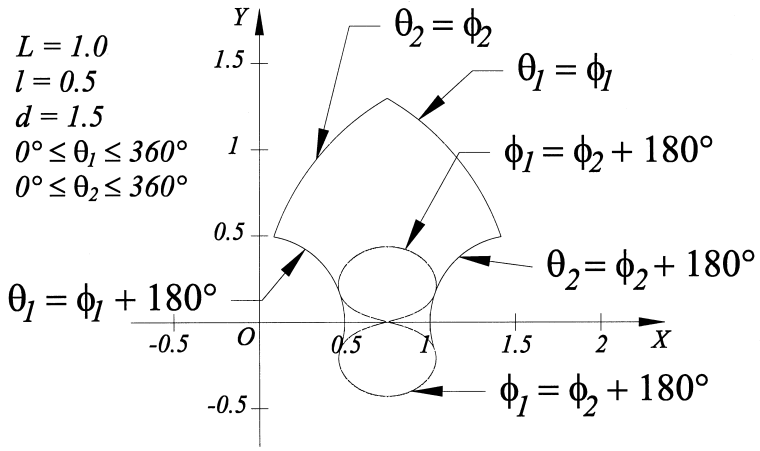

WS in Fig.12

Fig. 19. Singularity curves for $L = 1.0$, $l = 0.5$, $d = 1.5$, $0^\circ \le \theta_1 \le 360^\circ$ and $0^\circ \le \theta_2 \le 360^\circ$.

obtaining the results are not complicated and large, the computer being then capable of doing the simulation in an efficient way. Moreover, the capability of simultaneous generation of the reachable workspace and the singularity curves permits to obtain the effective workspace of the manipulator. Furthermore, physical insight and a considerable simplification were gained by means of the proposed branching identification and its corresponding relationship with the initial assembly configurations of the manipulator. In fact, the proposed branching identification helps to obtain the correct shape of the workspace.

References

[1] R. Akhras, J. Angeles, Mechanism and Machine Theory 25 (1) (1990) 97.
[2] G.H. Sutherland, N.R. Karwa, Mechanism and Machine Theory 13 (1978) 311.
[3] D.W. Lewis, C.K. Gyroy, Trans. A. J. Eng. Ind. Series B 89 (1967).
[4] J. Angeles, A. Alivizatos, R. Akhras, Mechanism and Machine Theory 23 (5) (1988) 343.
[5] Y. Nakamura, in: Advanced Robotics: Redundancy and Optimization, Addison-Wesley, 1991, p. 208.
[6] Y. Takeda, H. Funabashi, JSME International Journal 39 (1) (1996) 173.
[7] A.H. Soni, A.F. Vadasz, Transactions of the . ASME, (1977) 674.
[8] N.S. Davitashvili, Mechanism and Machine Theory 18 (6) (1983) 481.
[9] K.L. Ting, Transactions of the ASME, Journal of Mechanisms, Transmissions and Automation in Design 108 (1986) 533.
[10] K.L. Ting, Transactions of the ASME, Journal of Mechanisms, Transmissions and Automation in Design 111 (1989) 504.
[11] H. Asada, I.W. Ro, Transactions of the ASME, Journal of Mechanisms, Transmissions and Automation in Design 107 (1985) 536.
[12] Z. Shiller, S. Sundar, Transactions of the ASME, Journal of Mechanical Design 115 (1993) 199.
[13] G. Feng, Z.X. Qiu, Z.Y. Sheng, W.H. Rui, Mechanism and Machine Theory 31 (2) (1996) 173.
[14] B. Fallahi, H.Y. Lai, Y. Wang, Mechanism and Machine Theory 29 (5) (1994) 759.
[15] D. Sen, T.S. Mruthyunjaya, Mechanism and Machine Theory 33 (8) (1998) 1091.

[16] J. Angeles, A. Bernier, Transactions of the ASME, Journal of Mechanisms, Transmissions and Automation in Design 109 (1987) 197.
[17] S. Krishnamurty, D.A. Turcic, Transactions of the ASME, Journal of Mechanisms, Transmissions and Automation in Design 110 (1988) 414.
[18] D.T. Greenwood, in: Principles of Dynamics, second ed., Prentice-Hall, 1988, pp. 7–8.
[19] C. Gosselin, J. Angeles, Transactions of the ASME, Journal of Mechanical Design 112 (1990) 494.
[20] K.C. Gupta, in: Mechanics and Control of Robots, Springer, 1997, p. 51.